NUMERICAL SIMULATION OF DENSE GAS COMPRESSIBLE HOMOGENEOUS ISOTROPIC TURBULENCE

L. Sciacovelli[1,2], P. Cinnella[1,3]
[1] *DynFluid Laboratory, Arts et Métiers-ParisTech, Paris, France*
[2] *Dip. di Meccanica, Matematica e Management, Politecnico di Bari, Italy*
[3] *Dip. d'Ingeneria dell'innovazione, Università del Salento, Lecce, Italy*

Abstract The decay of compressible homogeneous isotropic turbulence for dense gases is studied by means of Direct Numerical Simulations and Implicit Large Eddy Simulations. A family of heavy fluorocarbons, which exhibit non-classical phenomena, is considered. The thermodynamic behavior of the fluids is modeled by the politropic Van der Waals or the five-term Virial Martin-Hou equations of state, and the results are compared to those obtained for a thermally and calorically perfect gas.

Turbulent flows of dense gases, i.e. gases with high molecular complexity working at thermodynamic conditions of the general order of magnitude of the liquid/vapor critical point, are of interest for a wide range of applications, including industrial and technological processes, aerospace propulsion or energy production. An interesting family of dense gases is represented by the so-called Bethe-Zel'dovich-Thompson (BZT) fluids, heavy polyatomic compounds characterized by a region of negative values of the Fundamental Derivative of Gas Dynamics Γ [10], in which non-classical phenomena such as rarefaction shock-waves, mixed shock/fan waves and shock splitting are expected to occur (e.g., see [2] and references therein). In this work, the impact of dense gas and BWT effects on the decay of Compressible Homogeneous Isotropic Turbulence (CHIT) is analysed, and the esults are compared with those obtained for perfect gases (PFG). Precisely, Implicit Large-Eddy Simulations (ILES) and DNS of dense gas CHIT are performed. The ILES approach consists in capturing the energy-containing and inertial ranges of turbulent flows, while relying on the numerical dissipation introduced by the discretization scheme to drain energy at subgrid scales. A tenth-order accurate centered scheme is used for the discretization of the convective fluxes. The scheme is supplemented by a high-order nonlinear artificial viscosity term, inspired from [6], that is 9th-order accurate in smooth flow regions and becomes 1st-order accurate near flow discontinuities. A Ducros-type sensor [4] is used to minimize the impact of artificial viscosity on the resolved vortical flow structures. The flow solver has been validated against literature results for both inviscid [5] and viscous [9] CHIT. To account for dense gas effects, the simple polytropic Van der Waals (VDW) equation of state (EoS) and the more complex Martin-Hou (MAH) EoS are used, in conjunction with a power law of the temperature for the specific heat at constant volume in the ideal gas limit. The VDW EoS is computationally inexpensive compared to more complex thermodynamic models, and provides a reasonable qualitative description of the main effects of interest. A simple power-law viscosity model is used for the VDW EoS, whereas the accurate Chung-Lee-Starling model [1], which takes into account correction terms for the dense gas region, is used in conjunction with the MAH EoS. The fluids under investigation belong to a family of heavy fluorocarbons, namely PP5 ($C_{10}F_{18}$), PP11 ($C_{14}F_{24}$) and PP25 ($C_{17}F_{30}$), which exhibit BZT effects for thermodynamic conditions near (but outside of) the critical region [3]. To initialize the isotropic turbulence field, divergence-free initial conditions with no density fluctuations were assumed. A Passot-Pouquet-type initial spectrum is considered and the peak wavenumber is fixed to $k_0 = 2$. Turbulent Mach numbers from 0.2 to 1.0 are investigated using mesh resolutions ranging from 64^3 to 512^3. Since the initialization is quasi-incompressible, for relatively high-Mach numbers an initial numerical transient is observed, where the compressible components of the turbulent structures increase and a physical state of fully developed turbulence is reached. For the chosen initial thermodynamic conditions, relatively close to the critical region, part of the flow evolves in the inversion zone. In this zone, the fluid compressibility exhibits large variations throughout the flow. This leads to large density and speed of sound fluctuations and to larger local values of the Mach number, and subsequently to remarkable differences in turbulence decay. High turbulent velocity fluctuations deriving from high turbulent Mach numbers lead to the occurrence of eddy shocklets [7], which strongly modify turbulence structure. In the neighborhood of eddy shocklets, indeed, the pressure is highly correlated with dilatation, and the production of dilatational dissipation increases, leading to a conversion of kinetic energy into internal energy. Actually, for BZT fluids working in regions where $\Gamma < 0$, the second law of thermodynamics requires that compression shocks cannot form; hence, locally, occurrence of compressive eddy shocklets is locally physically not admissible, whereas expansion shocklets are allowed. Fig. 1 shows a comparison between the turbulent kinetic energy decay for fluid PP11 modelled as a PFG or a VDW gas. At the beginning of the decay, viscous effects are small compared to nonlinear effects, and stronger shocklets originated in a PFG lead to additional dissipation and, subsequently, to a faster decay compared to the VDW case. Fig. 2 shows a comparison of the ratio of the local velocity divergence to its RMS value for fluid PP11 in PFG and VDW EoS. This quantity has been used ([9, 11]) to detect regions in which eddy shocklets may occur. In the VDW case, extremely strong expansion regions are present, whereas compressions are shown to be weaker than in the PFG case. The higher the molecular complexity of the fluid, the more non-classical phenomena became statistically important, since the BZT region is greater, leading to stronger variations of the speed of sound and, subsequently, of flow compressibility with density. These include non classical variations in flow regions $\Gamma < 0$, where the speed of sound descreases with increasing density. BZT effects results in a more symmetric distribution for the pdf of the local dilatation is obtained in the dense gas case (see Tab.1), and locally higher vorticity. Both of the thermodynamic models under investigation give similar qualitative results, even if the VDW models tends to overestimate dense gas effects with respect to the more realistic MAH model. Finally, a statical analysis of the turbulent structures is performed to show up the differences between dense and perfect gases. Precisely, a study in the plane of the second and third invariants of the anisotropic part of the deformation rate tensor is carried out. Preliminary results show that the universal behavior found in compressible and incompressible turbulence (i.e., [8]) is recovered also in the dense gas regime, as shown in Fig.2.

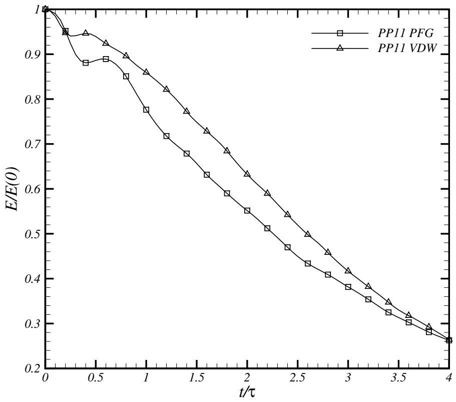

Figure 1: Turbulent kinetic energy decay.

θ/θ_{rms}	PFG	VDW
$[-\infty, -2.0]$	3.45%	2.53%
$[-2.0, -1.0]$	7.84%	9.58%
$[-1.0, 0.0]$	33.56%	38.21%
$[0.0, 1.0]$	44.88%	37.42%
$[1.0, 2.0]$	8.74%	9.54%
$[2.0, +\infty]$	1.53%	2.72%

Table 1: Percentage of volume occupied by flow regions with various dilatation levels at time $t = 4$.

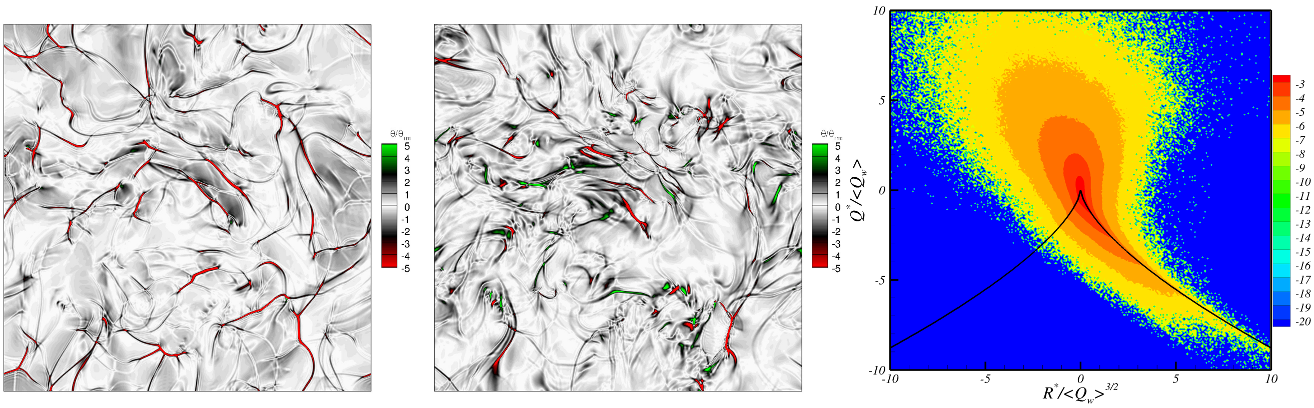

Figure 2: Ratio of dilatation to RMS dilatation for PFG EoS (left) and VDW EoS (center) for fluid PP9 at dimensionless time t=1. Right: $\log_{10}$ PDF (R*,Q*) for PP11 VDW case.

References

[1] T. H. Chung, M. Ajlan, L. L. Lee, and K. E. Starling. Generalized multiparameter correlation for nonpolar and polar fluid transport properties. *Industrial & engineering chemistry research*, **27**(4):671–679, 1988.

[2] P. Cinnella and P.M. Congedo. Inviscid and viscous aerodynamics of dense gases. *Journal of Fluid Mechanics*, **580**:179–217, 2007.

[3] MS Cramer. Negative nonlinearity in selected fluorocarbons. *Physics of Fluids A: Fluid Dynamics (1989-1993)*, **1**(11):1894–1897, 1989.

[4] F. Ducros, V. Ferrand, F. Nicoud, C. Weber, D. Darracq, C. Gacherieu, and T. Poinsot. Large-eddy simulation of the shock/turbulence interaction. *Journal of Computational Physics*, **152**(2):517–549, 1999.

[5] E. Garnier, M. Mossi, P. Sagaut, P. Comte, and M. Deville. On the use of shock-capturing schemes for large-eddy simulation. *Journal of Computational Physics*, **153**(2):273–311, 1999.

[6] J. W. Kim and D. J. Lee. Adaptive Nonlinear Artificial Dissipation Model for Computational Aeroacoustics. *AIAA Journal*, **39**:810–818, May 2001.

[7] S. Lee, S. K. Lele, and P. Moin. Eddy shocklets in decaying compressible turbulence. *Physics of Fluids A*, **3**:657, 1991.

[8] S. Pirozzoli and F. Grasso. Direct numerical simulations of isotropic compressible turbulence: Influence of compressibility on dynamics and structures. *Physics of Fluids (1994-present)*, **16**(12):4386–4407, 2004.

[9] R. Samtaney, D.I. Pullin, and B. Kosovic. Direct numerical simulation of decaying compressible turbulence and shocklet statistics. *Physics of Fluids*, **13**(5):1415–1430, 2001.

[10] P.A. Thompson. A Fundamental Derivative in Gas Dynamics. *Physics of Fluids*, **14**:1843–1849, 1971.

[11] J. Wang, Y. Shi, L. Wang, Z. Xiao, X.T. He, and S. Chen. Effect of compressibility on the small-scale structures in isotropic turbulence. *Journal of Fluid Mechanics*, **713**:588–631, 2012.